

Computational Design of Intrinsic Molecular Rectifiers Based on Asymmetric Functionalization of *N*-Phenylbenzamide

Wendu Ding,^{†,‡} Matthieu Koepp,[‡] Christopher Koenigsmann,[‡] Arunabh Batra,[§] Latha Venkataraman,^{*,§} Christian F. A. Negre,^{*,†,‡,||} Gary W. Brudvig,^{*,†,‡} Robert H. Crabtree,^{*,†,‡} Charles A. Schmuttenmaer,^{*,†,‡} and Victor S. Batista^{*,†,‡}

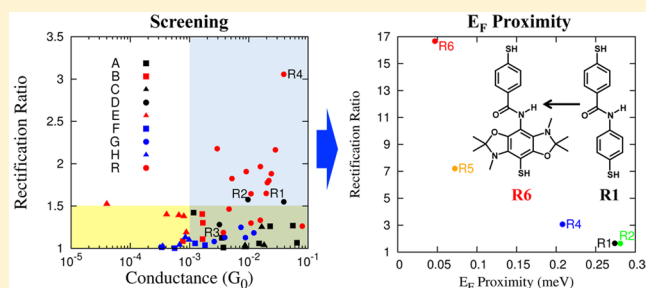
[†]Department of Chemistry, Yale University, P.O. Box 208107, New Haven, Connecticut 06520-8107, United States

[‡]Yale Energy Sciences Institute, Yale University, P.O. Box 27394, West Haven, Connecticut 06516-7394, United States

[§]Department of Applied Physics and Applied Mathematics, Columbia University, New York, New York 10027, United States

S Supporting Information

ABSTRACT: We report a systematic computational search of molecular frameworks for intrinsic rectification of electron transport. The screening of molecular rectifiers includes 52 molecules and conformers spanning over 9 series of structural motifs. *N*-Phenylbenzamide is found to be a promising framework with both suitable conductance and rectification properties. A targeted screening performed on 30 additional derivatives and conformers of *N*-phenylbenzamide yielded enhanced rectification based on asymmetric functionalization. We demonstrate that electron-donating substituent groups that maintain an asymmetric distribution of charge in the dominant transport channel (e.g., HOMO) enhance rectification by raising the channel closer to the Fermi level. These findings are particularly valuable for the design of molecular assemblies that could ensure directionality of electron transport in a wide range of applications, from molecular electronics to catalytic reactions.



INTRODUCTION

Molecular electronics has remained an attractive field of great interest since the seminal work of Mann and Kuhn in the early 1970s, which focused on conductance through monolayers of fatty acid salts.¹ Aviram and Ratner subsequently proposed that single molecules could be employed as discrete molecular devices for a broad range of applications.² However, for many years, advances in the field of molecular electronics were hindered by the complexity of examining the transport properties of single molecules at both the experimental and computational levels. Over the last two decades, new developments in single-molecule junction experimental techniques have allowed for reliable and reproducible measurements of molecular transport properties.^{3–12} Meanwhile, complementary developments in theoretical methods based on Green's function theory have also enabled more comprehensive examination of the fundamental properties of single molecules under nonequilibrium conditions.^{13–21}

Advances in studies of nonequilibrium transport properties of single molecules motivate the development of molecular motifs with transport properties tailored to a specific function. In nature, molecular assemblies are employed to induce directionality of electron transport in a variety of systems.²² In artificial systems, molecules could be equally wide-ranging as electronic components, including molecular wires, switches, diodes, and sensors. Compared with conventional electronics,

molecular structures offer several advantages, including their relatively small size (in the 1–100 nm range), the ability to tune function by tailoring chemical functionalities, and electronic/optical properties that can be tuned according to the molecular nature and their surrounding environment.²²

Molecular diodes are essential for current rectification at the molecular level.² In essence, molecular rectifiers allow more current to flow in one way than in reverse. The level of rectification can be quantified by the so-called “rectification ratio” ($RR = I^+/I^-$) defined as the ratio of forward (I^+) and reverse (I^-) currents, for a given bias potential applied forward and in reverse, respectively. Among the various possible applications, molecular rectifiers are expected to be particularly useful in photoelectrochemical cells that rely on efficient photoconversion at the single-molecule level.²³ Such rectifying components could suppress charge recombination which continues to be a long-standing challenge in organic photovoltaics^{24,25} and dye-sensitized photoelectrochemical devices.²⁶

A recent study of a Mn(II) redox-active center, anchored to TiO₂ via an *N*-phenylbenzamide linker,²³ has demonstrated the feasibility of suppressing back-electron transfer by suitable orientation of the amide functionality relative to the transport direction. Calculated current–voltage characteristic (I – V)

Received: August 26, 2015

curves for the $-\text{NHCO}-$ and $-\text{CONH}-$ orientations of the amide group yielded asymmetric I–V characteristics, consistent with electronic rectification as observed by the differing steady-state Mn(II)/Mn(III) ratios of the two orientations observed by EPR measurements. However, the reported level of rectification was very modest, and further work is required for computation design and characterization of molecular derivatives with much higher levels of rectification, as addressed in this study.

From a theoretical perspective, the current passing through a single molecule under bias can be obtained by integrating the transmission function, according to the Landauer–Büttiker formula.²⁷ Rectification arises whenever the integral of the transmission function is an asymmetric function of the applied voltage.²⁸ Based on a simple tight-binding model,¹⁰ eq 1, the transmission function $T(\epsilon, V)$ depends mainly on three voltage-dependent parameters, including the alignment of energy levels $\epsilon_0(V)$, as influenced by the Stark Effect within the molecular systems; the density of states of the electrodes $\text{DOS}_L(V)$ and $\text{DOS}_R(V)$ on the left and right side of the junction, respectively; and the couplings $\gamma_L(V)$ and $\gamma_R(V)$ between the molecule and the left and right contacts, respectively.²⁹

$$T(\epsilon, V) = \frac{4\pi^2\gamma_L^2(V)\text{DOS}_L(\epsilon, V)\gamma_R^2(V)\text{DOS}_R(\epsilon, V)}{[\epsilon - \epsilon(V)]^2 + \pi^2[\gamma_L^2(V)\text{DOS}_L(\epsilon, V) + \gamma_R^2(V)\text{DOS}_R(\epsilon, V)]^2} \quad (1)$$

The couplings $\gamma_L(V)$ and $\gamma_R(V)$ might be asymmetrically influenced by the forward and reverse applied bias potentials, inducing *extrinsic rectification*.^{30,31} Different anchoring groups on the left and right sides of the junction could also lead to different magnitudes of $\gamma_L(V)$ and $\gamma_R(V)$. Another way to induce extrinsic rectification is to use different electrodes on the left and right sides of the junction, providing different $\text{DOS}_L(V)$ and $\text{DOS}_R(V)$.³² In contrast, *intrinsic rectification* results from the distinct shift of the molecular energy levels $\epsilon_0(V)$ under forward, or reverse, applied bias potential.^{33,34} We focus on *intrinsic rectification* since it should be common to different systems with common molecular components.

Several recent advances have been reported in the field of electronic rectification by single molecules. Most molecular frameworks, however, either exhibit RRs smaller than 2 in the low bias region (<1 V)^{20,21,31,35,36} or show large RRs but were achieved through or in combination with extrinsic rectification.^{37–48} From a computational perspective, there have been relatively few examples of molecular candidates with intrinsic rectification,^{28,30,49–54} many of which, however, are very complex and hard to implement into molecular assemblies. Here, we analyze promising candidates from a library of 82 synthetically plausible molecules. Our computational screening protocol implements the nonequilibrium Green's function (NEGF) methodology, combined with density functional theory (DFT),^{55,56} as implemented in previous studies.^{23,29,57–60}

Such a methodology provides an efficient and reliable approach for the description of the electronic structure of molecular junctions under nonequilibrium conditions.

Our analysis shows that rectification correlates with the position of bands in the transmission function (TF) most proximal to the Fermi level (E_F) and with the asymmetry of the molecular orbital responsible for that peak determining the primary transport channel. These characteristics are consistent with prior reports^{20,21,28,31,52,61–66} and allow us to rationally

tailor the structure of new candidates investigated in this paper to generate molecular motifs with improved performance relative to the lead molecular structures.

COMPUTATIONAL METHODS

Molecular geometries were optimized at the DFT/B3LYP level⁶⁷ with the 6-31++G(d,p) basis set as implemented in Gaussian 09.⁶⁸ After optimization, thiol groups were deprotonated and covalently attached to gold contacts in the “atop” position. All S–Au distances were fixed at 2.32 Å,²⁹ and the gold contacts were modeled according to the Au nanocontact geometry, as described by Krstić et al.^{57–59} Each gold unit cell had two sublayers of either seven or three gold atoms with periodic boundary conditions along the transport direction. Transport properties were computed by using the extended three-system model, shown in Figure 1. An extra 7-atom layer is

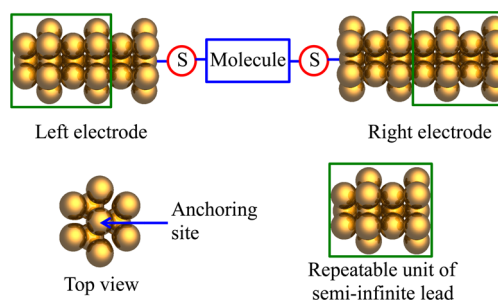


Figure 1. Three-system model (extended molecule) used to compute transport properties of single molecules (blue box) connected to gold contacts via thiolate groups, denoted by red circles. Green boxes indicate the unit cells for the leads. We employed the Au lattice constant of 4.088 Å in an hcp lattice. The face of the leads corresponds to a (111) surface.^{57–59}

inserted between the molecule and the right lead to ensure the same attachment of the molecule to the left and right leads. This type of lead provides robust results comparable to those using more complex models.²⁹ Meanwhile, because of its simplicity, the computational cost can be significantly reduced on the screening process. Since the transport is dependent on the local geometry of the molecule-electrode contact,^{15,16,19,60,69} the main focus should be placed on the trends of transport properties that exist among the candidate molecules, rather than the absolute numbers.

The I–V curves were computed by using the DFT-NEGF approach, as implemented in the TranSIESTA computational package.⁵⁶ For calculation efficiency, the geometries of the molecules were not allowed to vary with the bias. However, the effect of applied bias on the molecular geometry can be neglected when the applied bias is small.⁷⁰ A double- ζ basis set⁷¹ was used for all transport calculations, which is sufficient to describe the dominant energy levels involved in electron transport. The generalized gradient approximation (GGA)⁷² was used as the exchange correlation functional. To sample the Brillouin zone, we used the gamma point for the extended molecular region and a $1 \times 1 \times 80$ Monkhorst–Pack k -point grid for the leads. The energy cutoff for the real space grid was 200 Ry. The rectification ratio was obtained from currents calculated at ± 0.2 V. Although the selection of the bias is arbitrary, recent results suggest that the RR values obtained at 0.2 V are most consistent with those measured experimentally by the scanning tunneling microscopy break junction technique.³¹

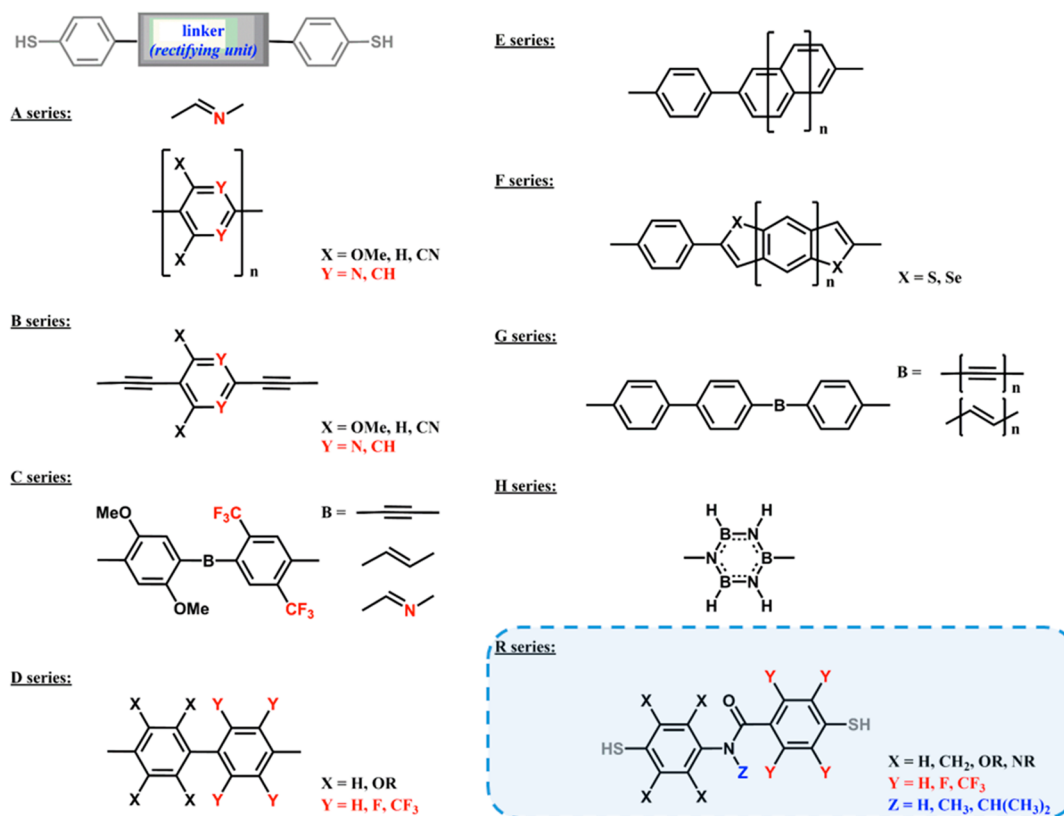


Figure 2. Molecular motifs computationally screened for rectification. All cases except series R were computed with a *p*-mercaptophenyl group bonded to each end of the molecule. Series R were computed as drawn in the figure.

Figure 2 shows the molecular motifs analyzed in this study which were chosen according to synthetic plausibility, excluding other candidates on the basis of toxicity of the target compound, commercial availability of the precursors, and chemical stability of the targeted structure under working conditions. Although these criteria excluded a large number of otherwise attractive structures, our strategy facilitates rapid experimental testing of the most promising candidates selected by computational screening.

Initial lead molecules were derived from structures that showed *in silico* rectification at the single molecule level.^{34,73} Others were derived from earlier work on the *N*-phenylbenzamide and stilbene bridges²⁹ and architectures based on the “donor/acceptor” design introduced by Aviram and Ratner² and later developed by Metzger and co-workers.⁷⁴

Among the various different categories of probed molecular frameworks, we highlight compact polarized π -systems that are partly or fully conjugated with their anchoring groups (Figure 2 series A and B, respectively); weakly or highly conjugated biphenyls derivatives featuring “donor/acceptor” character (series C and D, respectively); asymmetric π -systems associating two segments of different polarizability (series E, F, and G); derivatives of borazine (series H); and derivatives of the *N*-phenylbenzamide bridge whose structure is modulated by various substituents on the phenylene groups and/or the nitrogen of the amide (series R). Overall, we explored 82 molecules in order to find the best candidates for both high rectification and conductance.

RESULTS AND DISCUSSION

Figure 3 reports the calculated RRs as a function of the calculated single molecule conductance for 52 synthetically plausible

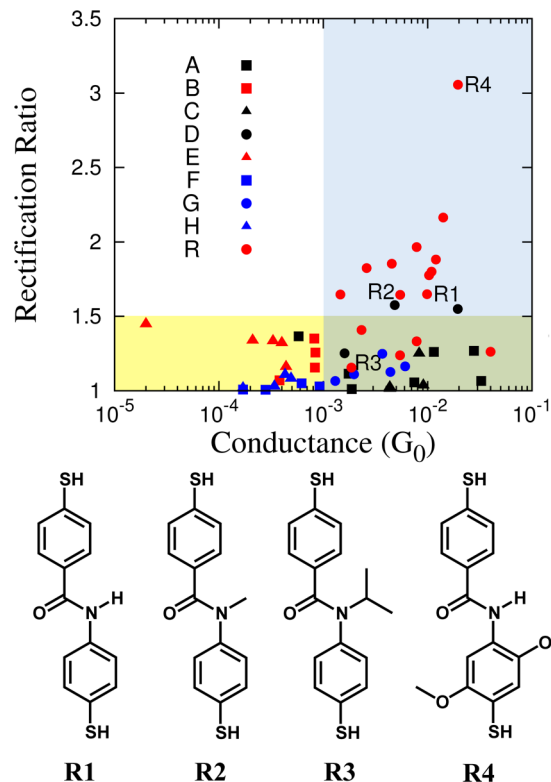


Figure 3. Calculated RR versus conductance on a semilog scale for 52 synthetically plausible molecular candidates and conformers spanning the structural motifs shown in Figure 2. Molecular structures of R1, R2, R3, and R4 are shown in the lower panel.

Table 1. Calculated Values of Conductance (G) and RRs for Molecules Analyzed in This Work

molecules	G (G_0)	RR ^a
R1	9.9×10^{-3}	1.65
R2	5.5×10^{-3}	1.64
R3	1.9×10^{-3}	1.19
R4	2.0×10^{-2}	3.06
R5	7.8×10^{-3}	7.20
R6	9.1×10^{-5}	16.67

^aThe rectification ratio is measured at a bias of 0.2 V.

molecules and conformers spanning the structural motifs shown in Figure 2. With the exception of structures derived from the *N*-phenylbenzamide backbone (series R), we observe that it is rather uncommon for a molecule to exhibit both high

rectification and high conductance. Three groups of molecules presenting similar characteristics can be distinguished: those with low rectification and low conductance (yellow area); low RR and high conductance (green); and high RR and high conductance (blue), which are the candidates of interest. Compared to the rest of the candidates screened, *N*-phenylbenzamide-based architectures (series R) are generally expected to exhibit remarkably good rectifying and conducting properties, as shown in the upper right corner of Figure 3 (blue). The calculated conductance and RR for selected molecules from series R are summarized in Table 1.

Compared to other molecular motifs, the *N*-phenylbenzamide core (R1, Figure 3) has a very simple molecular structure and was predicted by calculations to have both an attractive rectification ratio (RR = 1.65) and a high conductance of $9.9 \times 10^{-3} G_0$ (see Table 1). R1 is expected to exhibit both intrinsic

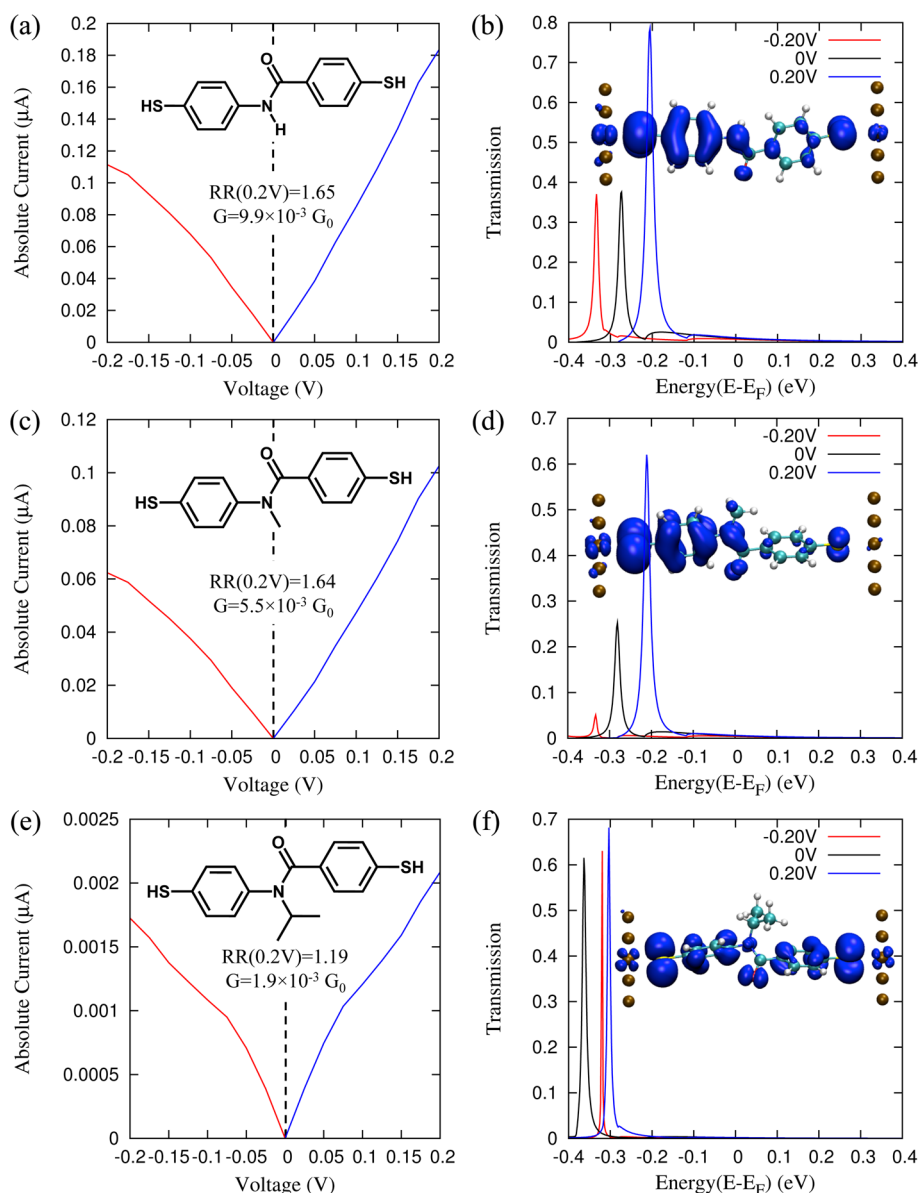


Figure 4. Calculated electron-transport properties of molecules R1, R2, and R3, including the I–V curves with absolute current (a, c, and e) and transmission functions (b, d, and f) for R1 (a and b), R2 (c and d), and R3 (e and f). The insets of panels b, d, and f show iso-surfaces of projected DOS of transport channels, showing that channels localized on one side of the junction (b and d) have higher rectification than delocalized channels (f), as shown by the corresponding I–V curves.

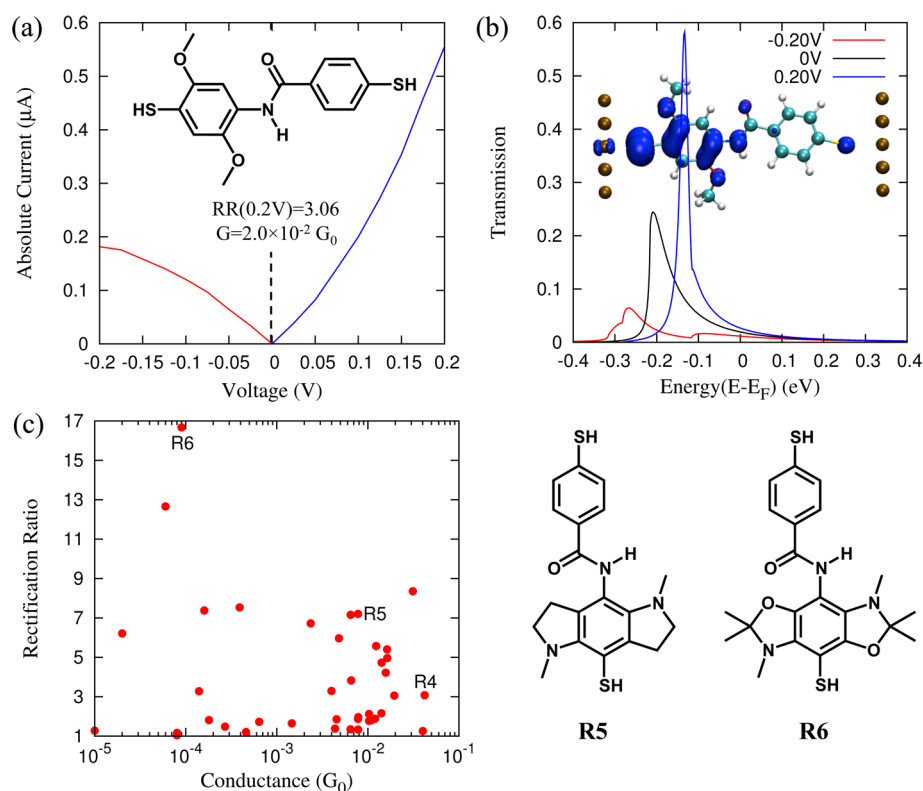


Figure 5. Calculated electron-transport properties for molecule **R4**, including the I–V curve with absolute current (a) and transmission function (b). The inset of (b) show the localized DOS projected onto the states of the transmitting peak. (c) Calculated RR versus conductance on a semilog scale for an additional 30 molecular candidates and conformers further modified based on **R4**, in addition to 10 molecules from our original screening which have similar structures as **R4**. Molecular structures of two examples, **R5** and **R6**, are shown in the right panel of (c).

and early rectification at low to moderate voltages, as suggested by a previous theoretical study.²⁹ The preferred direction for electron flow in this type of amide system is from N to CO in the –NHCO– direction (i.e., from the aniline to the benzoyl-fragment). The main transmission peak, next to the Fermi level (E_F), corresponds to the HOMO (inset Figure 4(b)) and is, therefore, assigned as the main transport channel. The HOMO is localized on the aniline side of the *N*-phenylbenzamide core. Due to the underlying asymmetry, the HOMO energy is raised closer to the Fermi level when the potential of the electrode connected to the aniline ring is raised under forward bias, while it is lowered and shifted away from E_F under reverse bias potentials (Figure 4(b)). As a result of the shift in energy, the area under the transmission function within the integration window ($E_F - V/2$, $E_F + V/2$) is increased for forward bias potentials and decreased for reverse bias voltages, accounting for the calculated asymmetry of I–V curves shown in Figure 4(a). The same effect was observed for a rotamer of stilbene in which the HOMO orbital was localized on only one side of the molecule.²⁹ These findings suggest that rational design of molecular rectifiers is possible through localization of the frontier orbital responsible for the transport channel on one side of the molecular junction by either introducing donor–acceptor groups or conformational constraints.

To test the validity of the aforementioned mechanism (low bias rectification), we analyzed two other molecular derivatives of compound **R1**. These molecules are the *N*-methyl (**R2**) and *N*-isopropyl (**R3**) derivatives of the parent *N*-phenylbenzamide core (see Figure 3). These two molecules have a framework very similar to **R1** but very different electron transport properties. In the case of **R2**, the dihedral angle between the

phenyl and the carbonyl group is increased to 40° as compared to 24° in **R1**, and the overall twist angle between the two phenyl rings increases to almost 90° (inset of Figure 4(d)). The broken conjugation leads to a 2-fold current reduction ($G = 5.5 \times 10^{-3} G_0$ for **R2**) with respect to **R1**. However, the orthogonality between the two phenylene planes does not change the localization of the transmission state (i.e., the symmetry of the HOMO). As a consequence, the RR calculated for **R2** (1.64 at 0.2 V) remains similar to the value calculated for **R1** (see I–V curves shown in Figure 4(a) and (c)). Figure 4(d) shows the transmission peak shifting toward and away from the E_F as the bias is swept positively and negatively, respectively, in the same manner as previously reported for **R1**. This provides further evidence that the predominant transport channel is primarily related to the HOMO of the *N*-phenylbenzamide core.

In the case of **R3**, the two phenylene rings are forced to orient largely orthogonal to the amide bond motif due to the high steric crowding introduced by the isopropyl substituent, which is in contrast to **R1** and **R2** (see Figure S2 in the SI for dihedral angles). The orthogonality breaks the extended conjugation between the left phenylene group and the amide bond. Therefore, there is no significant energy difference between the left and the right rings, providing equal residing probability for electrons with corresponding energies. As a result, the HOMO is effectively delocalized over the entire molecule, and **R3** exhibits almost no rectification since the transmission peak shifts in the same direction regardless of the direction of the applied bias. From the I–V curve of **R3**, the RR is predicted to be 1.19 at 0.2 V, which is significantly lower than that of **R1** and **R2**. Furthermore, the decreased conjugation

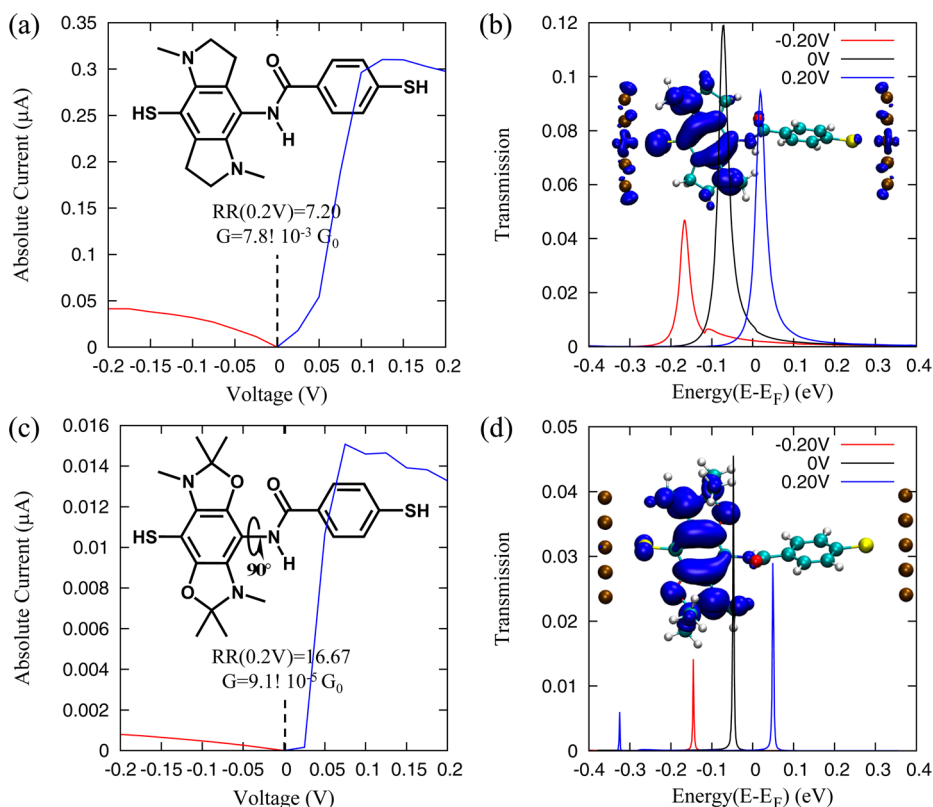


Figure 6. Calculated electron-transport properties for molecules **R5** and **R6**, including the I–V curves with absolute current (a and c) and transmission function (b and d) for **R5** (a and b) and **R6** (c and d). The insets of (b) and (d) show the localized DOS projected onto the states of the transmitting peak.

causes the conductance to drop to a value of $1.9 \times 10^{-3} G_0$, which is lower than both **R1** and **R2**.

The reported results show that electronic rectification can be traced back to the asymmetry of the transmission channel along the transport path, which is usually the longest axis of the molecular bridge. For the molecules investigated in our study, based on *N*-phenylbenzamide backbones, the transmission state has a predominant HOMO character. Therefore, structures with a HOMO localized on one side of the amide bridge have higher rectification.

The most promising candidate from the initial screening is compound **R4**, a derivative of **R1** with two methoxy substituent groups introduced into the aniline group (see Figure 3). This compound exhibits a calculated RR of 3.06, which is much higher than that of **R1** and **R2**. The electron donating methoxy groups raise the HOMO of **R4** closer to E_F , therefore achieving earlier rectification and higher RR under low bias. Figure 5 shows that the transmission function and I–V curve for **R4**, with a transmission resonance located at -0.21 eV, which is about 70 mV closer to E_F than the corresponding transport channels of **R1** and **R2**. As a result, the area under the transmission function within the integration window is larger (e.g., for an applied bias of 200 mV) and changes more dramatically for positive and negative bias potentials, thereby explaining the large RR. The proximity of the transport channel to the Fermi level, referred to here as “ E_F proximity”, amplifies the asymmetric response since it increases the integral of the transmission function over the energy range ($E_F - V/2, E_F + V/2$).

Given the promising results for **R4**, we have investigated additional modifications of the *N*-phenylbenzamide backbone and introduced highly electron-donating groups to further

increase the E_F proximity effect. Using the same screening method, we obtain the results shown in Figure 5(c). A total of 30 molecules and conformers were included in this second screening, all of which are derivatives of **R4** with different number and types of functionalization on the aniline group, both symmetrical and unsymmetrical. These substituents include alkyl groups, alkoxy groups, secondary, and tertiary amines, etc. Two molecules from the screening (**R5** and **R6**, see Figure 5(c)) have been selected for analysis, as they exhibit structural similarity to **R4** and display either high conductance or higher RR.

In **R5** (see Figure 6(a)), amines were introduced into the five-membered rings to ensure the most efficient coupling between the lone pair of the nitrogen atom and the π -system of the phenylene ring. Figure 6(b) shows that the electron-donating groups in **R5** shift the transmission channel to about -72 meV, which is significantly closer to the Fermi level than for **R4** (-210 meV). We note that for a positive bias, starting from a bias of 0.1 V, the entire transmission peak is located inside the integration window, while for a negative bias, only a small tail remains in the integration window. Accordingly, the predicted rectification increases significantly to a RR = 7.2 and is observed earlier (peaks at 125 mV, compared to **R1**, **R2**, and **R4** at 200 mV), indicating that this compound is a promising candidate for the design of compact rectifying bridges. In **R6**, additional oxygen atoms are introduced into the cyclic amines in **R5** (see Figure 6(c)). This substitution further raises the dominant transmission peak of the molecule to -47 meV toward the Fermi level (see Figure 6(d)). In addition, due to the broken conjugation, the transmission peak is narrowed, which creates a more pronounced change on the current when

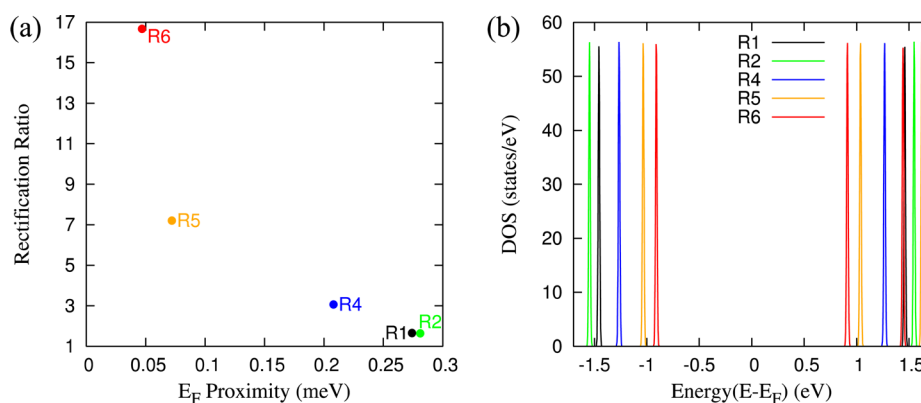


Figure 7. (a) Correlation between RR and E_F proximity. (b) Energy levels of frontier orbitals of R1, R2, R4, R5, and R6. All E_F (middle of HOMO–LUMO gap) are set to 0.000 eV to facilitate comparison.

moving in or out of the transport window. Consequently, the RR at 0.2 V of R6 is dramatically increased to a value of 16.67 and has a peak at 75 mV. However, the conductance is reduced more than 2 orders of magnitude to $9.1 \times 10^{-5} G_0$, due to steric effects.

These results are best illustrated in Figure 7(a) where it is obvious that the smaller the E_F proximity, the larger the RR is. The irregular change of RR with E_F proximity can be attributed to differences in the molecule–electrode couplings, as shown by the different widths of the transmission functions for various different molecules.

We note that the proximity of the HOMO to the Fermi level is correlated with a decreasing HOMO–LUMO gap for the isolated molecule (see Figure 7(b)), which follows the trend of R2 (3.096 eV) > R1 (2.916 eV) > R4 (2.532 eV) > R5 (2.072 eV) > R6 (1.823 eV). This trend is preserved for the compounds coupled to the gold contacts, suggesting that HOMO–LUMO gaps in conjunction with the asymmetry of the frontier orbitals for the isolated molecules could provide simple guidelines for optimization of rectification properties. At the same time, we note that although decoupling between molecule and the electrodes enhances rectification, it is balanced with the trade-off of lower overall conductance.

CONCLUSIONS

We have identified *N*-phenylbenzamide derivatives, as promising scaffolds for intrinsic molecular rectifiers, as predicted by a computational screening methodology based on DFT-NEGF calculations. Extensive computational screening of synthetically plausible molecular motifs shows that the amide group provides both high rectification and high conductance. We find that rectification can be enhanced by electron-donating functional groups that shift the HOMO of *N*-phenylbenzamide derivatives closer to the Fermi level. The analysis of derivatives with different modifications of the aniline group determined a fundamental relationship between the electronic properties of the molecules and their corresponding rectification ability. To increase the RR under low bias, the dominant transport state must be positioned as close as possible to the Fermi level of the contacts and must have an asymmetric distribution of electronic density. The optimal level alignment and asymmetry of such a frontier orbital can, therefore, be tailored with suitable electron-donating (or electron-withdrawing) groups, as demonstrated in this study. Promising molecular rectifiers, with RR = 3.06 for R4, RR = 7.20 for R5, and RR = 16.67 for R6 at 200 mV, have

been computationally designed with a suitable choice of substituents on the *N*-phenylbenzamide core.

ASSOCIATED CONTENT

Supporting Information

The Supporting Information is available free of charge on the ACS Publications website at DOI: 10.1021/acs.jctc.5b00823.

Description of gold contact used for calculations; flowchart of computational screening procedure; structures and collective data of transport properties of the 82 molecules screened in this work; sample input files for leads calculation and transport calculations (PDF)

AUTHOR INFORMATION

Corresponding Authors

- *E-mail: lv2117@columbia.edu (L.V.)
- *E-mail: christianfannegre@gmail.com (C.F.A.N.)
- *E-mail: gary.brudvig@yale.edu (G.W.B.)
- *E-mail: robert.crabtree@yale.edu (R.H.C.)
- *E-mail: charles.schmuttermaer@yale.edu (C.A.S.)
- *E-mail: victor.batista@yale.edu (V.S.B.)

Present Address

^{||}Theoretical Division, Los Alamos National Laboratory, Los Alamos, New Mexico 87545, United States.

Notes

The authors declare no competing financial interest.

ACKNOWLEDGMENTS

This work was funded by the U.S. Department of Energy, Office of Science, Office of Basic Energy Sciences under Award Number DE-FG02-07ER15909 and a generous gift from the TomKat Charitable Trust. V.S.B. acknowledges computational resources from NERSC and from the Yale University Faculty of Arts and Sciences High Performance Computing Center partially, funded by the National Science Foundation grant CNS 08-21132. L.V. thanks the Packard Foundation for support. A.B. was supported by the NSF GRFP Grant No. DGE-07-07425.

REFERENCES

- (1) Mann, B.; Kuhn, H. Tunneling through Fatty Acid Salt Monolayers. *J. Appl. Phys.* **1971**, *42*, 4398–4405.
- (2) Aviram, A.; Ratner, M. A. Molecular rectifiers. *Chem. Phys. Lett.* **1974**, *29*, 277–283.

- (3) Reed, M. A.; Zhou, C.; Muller, C. J.; Burgin, T. P.; Tour, J. M. Conductance of a Molecular Junction. *Science* **1997**, *278*, 252–254.
- (4) Liang, W.; Shores, M. P.; Bockrath, M.; Long, J. R.; Park, H. Kondo resonance in a single-molecule transistor. *Nature* **2002**, *417*, 725–729.
- (5) Park, J.; Pasupathy, A. N.; Goldsmith, J. I.; Chang, C.; Yaish, Y.; Petta, J. R.; Rinkoski, M.; Sethna, J. P.; Abruna, H. D.; McEuen, P. L.; Ralph, D. C. Coulomb blockade and the Kondo effect in single-atom transistors. *Nature* **2002**, *417*, 722–725.
- (6) Xu, B.; Tao, N. J. Measurement of Single-Molecule Resistance by Repeated Formation of Molecular Junctions. *Science* **2003**, *301*, 1221–1223.
- (7) Xiao, X.; Xu, B.; Tao, N. J. Measurement of Single Molecule Conductance: Benzenedithiol and Benzenedimethanethiol. *Nano Lett.* **2004**, *4*, 267–271.
- (8) Venkataraman, L.; Klare, J. E.; Tam, I. W.; Nuckolls, C.; Hybertsen, M. S.; Steigerwald, M. L. Single-Molecule Circuits with Well-Defined Molecular Conductance. *Nano Lett.* **2006**, *6*, 458–462.
- (9) McCreery, R. L.; Bergren, A. J. Progress with Molecular Electronic Junctions: Meeting Experimental Challenges in Design and Fabrication. *Adv. Mater.* **2009**, *21*, 4303–4322.
- (10) Cuevas, J. C.; Scheer, E. *Molecular Electronics: An Introduction to Theory and Experiment*; World Scientific Publishing Company Pte Limited: 2010.
- (11) Kaliginedi, V.; Moreno-García, P.; Valkenier, H.; Hong, W.; García-Suárez, V. M.; Buiterr, P.; Otten, J. L. H.; Hummelen, J. C.; Lambert, C. J.; Wandlowski, T. Correlations between Molecular Structure and Single-Junction Conductance: A Case Study with Oligo(phenylene-ethynylene)-Type Wires. *J. Am. Chem. Soc.* **2012**, *134*, 5262–5275.
- (12) Aradhya, S. V.; Venkataraman, L. Single-molecule junctions beyond electronic transport. *Nat. Nanotechnol.* **2013**, *8*, 399–410.
- (13) Xue, Y.; Datta, S.; Ratner, M. A. First-principles based matrix Green's function approach to molecular electronic devices: general formalism. *Chem. Phys.* **2002**, *281*, 151–170.
- (14) Jones, D. R.; Troisi, A. Single Molecule Conductance of Linear Dithioalkanes in the Liquid Phase: Apparently Activated Transport Due to Conformational Flexibility. *J. Phys. Chem. C* **2007**, *111*, 14567–14573.
- (15) Quek, S. Y.; Venkataraman, L.; Choi, H. J.; Louie, S. G.; Hybertsen, M. S.; Neaton, J. B. Amine–Gold Linked Single-Molecule Circuits: Experiment and Theory. *Nano Lett.* **2007**, *7*, 3477–3482.
- (16) Paulsson, M.; Krag, C.; Frederiksen, T.; Brandbyge, M. Conductance of Alkanedithiol Single-Molecule Junctions: A Molecular Dynamics Study. *Nano Lett.* **2009**, *9*, 117–121.
- (17) Quek, S. Y.; Choi, H. J.; Louie, S. G.; Neaton, J. B. Length Dependence of Conductance in Aromatic Single-Molecule Junctions. *Nano Lett.* **2009**, *9*, 3949–3953.
- (18) Strange, M.; Thygesen, K. S. Towards quantitative accuracy in first-principles transport calculations: The GW method applied to alkane/gold junctions. *Beilstein J. Nanotechnol.* **2011**, *2*, 746–754.
- (19) Darancet, P.; Widawsky, J. R.; Choi, H. J.; Venkataraman, L.; Neaton, J. B. Quantitative Current–Voltage Characteristics in Molecular Junctions from First Principles. *Nano Lett.* **2012**, *12*, 6250–6254.
- (20) Williams, P. D.; Reuter, M. G. Level Alignments and Coupling Strengths in Conductance Histograms: The Information Content of a Single Channel Peak. *J. Phys. Chem. C* **2013**, *117*, 5937–5942.
- (21) Kim, T.; Darancet, P.; Widawsky, J. R.; Kotiuga, M.; Quek, S. Y.; Neaton, J. B.; Venkataraman, L. Determination of Energy Level Alignment and Coupling Strength in 4,4'-Bipyridine Single-Molecule Junctions. *Nano Lett.* **2014**, *14*, 794–798.
- (22) Heath, J. R.; Ratner, M. A. Molecular electronics. *Phys. Today* **2003**, *56*, 43–49.
- (23) Ding, W.; Negre, C. F. A.; Palma, J. L.; Durrell, A. C.; Allen, L. J.; Young, K. J.; Milot, R. L.; Schmuttenmaer, C. A.; Brudvig, G. W.; Crabtree, R. H.; Batista, V. S. Linker Rectifiers for Covalent Attachment of Transition-Metal Catalysts to Metal-Oxide Surfaces. *ChemPhysChem* **2014**, *15*, 1138–1147.
- (24) Tamura, H.; Burghardt, I. Ultrafast Charge Separation in Organic Photovoltaics Enhanced by Charge Delocalization and Vibronically Hot Exciton Dissociation. *J. Am. Chem. Soc.* **2013**, *135*, 16364–16367.
- (25) Giazitzidis, P.; Argyrakis, P.; Bisquert, J.; Vikhrenko, V. S. Charge separation in organic photovoltaic cells. *Org. Electron.* **2014**, *15*, 1043–1049.
- (26) O'Regan, B.; Gratzel, M. A Low-Cost, High-Efficiency Solar-Cell Based on Dye-Sensitized Colloidal TiO₂ Films. *Nature* **1991**, *353*, 737–740.
- (27) Landauer, R. Electrical resistance of disordered one-dimensional lattices. *Philos. Mag.* **1970**, *21*, 863–867.
- (28) Mujica, V.; Ratner, M. A.; Nitzan, A. Molecular rectification: why is it so rare? *Chem. Phys.* **2002**, *281*, 147–150.
- (29) Ding, W.; Negre, C. F. A.; Vogt, L.; Batista, V. S. Single Molecule Rectification Induced by the Asymmetry of a Single Frontier Orbital. *J. Chem. Theory Comput.* **2014**, *10*, 3393–3400.
- (30) Taylor, J.; Brandbyge, M.; Stokbro, K. Theory of Rectification in Tour Wires: The Role of Electrode Coupling. *Phys. Rev. Lett.* **2002**, *89*, 138301.
- (31) Batra, A.; Darancet, P.; Chen, Q.; Meisner, J. S.; Widawsky, J. R.; Neaton, J. B.; Nuckolls, C.; Venkataraman, L. Tuning Rectification in Single-Molecular Diodes. *Nano Lett.* **2013**, *13*, 6233–6237.
- (32) Pan, J. B.; Zhang, Z. H.; Ding, K. H.; Deng, X. Q.; Guo, C. Current rectification induced by asymmetrical electrode materials in a molecular device. *Appl. Phys. Lett.* **2011**, *98*, 092102.
- (33) Elbing, M.; Ochs, R.; Koentopp, M.; Fischer, M.; von Hänisch, C.; Weigend, F.; Evers, F.; Weber, H. B.; Mayor, M. A single-molecule diode. *Proc. Natl. Acad. Sci. U. S. A.* **2005**, *102*, 8815–8820.
- (34) Díez-Pérez, I.; Hihath, J.; Lee, Y.; Yu, L.; Adamska, L.; Kozhushner, M. A.; Oleynik, I. I.; Tao, N. Rectification and stability of a single molecular diode with controlled orientation. *Nat. Chem.* **2009**, *1*, 635–641.
- (35) Meisner, J. S.; Ahn, S.; Aradhya, S. V.; Krikorian, M.; Parameswaran, R.; Steigerwald, M.; Venkataraman, L.; Nuckolls, C. Importance of Direct Metal– π Coupling in Electronic Transport Through Conjugated Single-Molecule Junctions. *J. Am. Chem. Soc.* **2012**, *134*, 20440–20445.
- (36) Yee, S. K.; Sun, J.; Darancet, P.; Tilley, T. D.; Majumdar, A.; Neaton, J. B.; Segalman, R. A. Inverse Rectification in Donor–Acceptor Molecular Heterojunctions. *ACS Nano* **2011**, *5*, 9256–9263.
- (37) Capozzi, B.; Xia, J.; Adak, O.; Dell, E. J.; Liu, Z.-F.; Taylor, J. C.; Neaton, J. B.; Campos, L. M.; Venkataraman, L. Single-molecule diodes with high rectification ratios through environmental control. *Nat. Nanotechnol.* **2015**, *10*, 522–527.
- (38) Van Dyck, C.; Ratner, M. A. Molecular Rectifiers: A New Design Based on Asymmetric Anchoring Moieties. *Nano Lett.* **2015**, *15*, 1577–1584.
- (39) Ma, J.; Yang, C.-L.; Wang, M.-S.; Ma, X.-G. Controlling the electronic transport properties of the tetrapyrimidinyl molecule with atom modified sulfur bridge. *RSC Adv.* **2015**, *5*, 10675–10679.
- (40) Garg, K.; Majumder, C.; Nayak, S. K.; Aswal, D. K.; Gupta, S. K.; Chattopadhyay, S. Silicon-pyrene/perylene hybrids as molecular rectifiers. *Phys. Chem. Chem. Phys.* **2015**, *17*, 1891–1899.
- (41) Li, J.; Zhang, Z. H.; Qiu, M.; Yuan, C.; Deng, X. Q.; Fan, Z. Q.; Tang, G. P.; Liang, B. High-performance current rectification in a molecular device with doped graphene electrodes. *Carbon* **2014**, *80*, 575–582.
- (42) Yoon, H. J.; Liao, K.-C.; Lockett, M. R.; Kwok, S. W.; Baghbanzadeh, M.; Whitesides, G. M. Rectification in Tunneling Junctions: 2,2'-Bipyridyl-Terminated n-Alkanethiolates. *J. Am. Chem. Soc.* **2014**, *136*, 17155–17162.
- (43) Fu, X.-X.; Zhang, R.-Q.; Zhang, G.-P.; Li, Z.-L. Rectifying Properties of Oligo(Phenylene Ethynylene) Heterometallic Molecular Junctions: Molecular Length and Side Group Effects. *Sci. Rep.* **2014**, *4*, 6357.
- (44) Song, Y.; Xie, Z.; Ma, Y.; Li, Z.-L.; Wang, C.-K. Giant Rectification Ratios of Azulene-like Dipole Molecular Junctions

Induced by Chemical Doping in Armchair-Edged Graphene Nanoribbon Electrodes. *J. Phys. Chem. C* **2014**, *118*, 18713–18720.

(45) Wang, K.; Zhou, J.; Hamill, J. M.; Xu, B. Measurement and understanding of single-molecule break junction rectification caused by asymmetric contacts. *J. Chem. Phys.* **2014**, *141*, 054712.

(46) Kim, T.; Liu, Z.-F.; Lee, C.; Neaton, J. B.; Venkataraman, L. Charge transport and rectification in molecular junctions formed with carbon-based electrodes. *Proc. Natl. Acad. Sci. U. S. A.* **2014**, *111*, 10928–10932.

(47) Batra, A.; Meisner, J. S.; Darancet, P.; Chen, Q.; Steigerwald, M. L.; Nuckolls, C.; Venkataraman, L. Molecular diodes enabled by quantum interference. *Faraday Discuss.* **2014**, *174*, 79–89.

(48) Sherif, S.; Rubio-Bollinger, G.; Pinilla-Cienfuegos, E.; Coronado, E.; Cuevas, J. C.; Agraït, N. Current rectification in a single molecule diode: the role of electrode coupling. *Nanotechnology* **2015**, *26*, 291001.

(49) Andrews, D. Q.; Solomon, G. C.; Van Duyne, R. P.; Ratner, M. A. Single Molecule Electronics: Increasing Dynamic Range and Switching Speed Using Cross-Conjugated Species. *J. Am. Chem. Soc.* **2008**, *130*, 17309–17319.

(50) Yang, Z.; Ji, Y.-L.; Lan, G.; Xu, L.-C.; Liu, X.; Xu, B. Design molecular rectifier and photodetector with all-boron fullerene. *Solid State Commun.* **2015**, *217*, 38–42.

(51) Lei, H.; Tan, X.-Q. A Theoretical Investigation on Rectifying Performance of a Single Motor Molecular Device. *Chin. Phys. Lett.* **2015**, *32*, 027302.

(52) Tsuji, Y.; Yoshizawa, K. Current Rectification through π - π Stacking in Multilayered Donor–Acceptor Cyclophanes. *J. Phys. Chem. C* **2012**, *116*, 26625–26635.

(53) Liu, H.; He, Y.; Zhang, J.; Zhao, J.; Chen, L. A theoretical study of asymmetric electron transport through linearly aromatic molecules. *Phys. Chem. Chem. Phys.* **2015**, *17*, 4558–4568.

(54) Montiel, F.; Fomina, L.; Fomine, S. Charge transfer complexes of fullerene[60] with porphyrins as molecular rectifiers. A theoretical study. *J. Mol. Model.* **2015**, *21*, 1–8.

(55) Rocha, A. R.; Garcia-Suarez, V. M.; Bailey, S. W.; Lambert, C. J.; Ferrer, J.; Sanvito, S. Towards molecular spintronics. *Nat. Mater.* **2005**, *4*, 335–339.

(56) Brandbyge, M.; Mozos, J.-L.; Ordejón, P.; Taylor, J.; Stokbro, K. Density-functional method for nonequilibrium electron transport. *Phys. Rev. B: Condens. Matter Mater. Phys.* **2002**, *65*, 165401.

(57) Krstić, P.; Zhang, X. G.; Butler, W. Generalized conductance formula for the multiband tight-binding model. *Phys. Rev. B: Condens. Matter Mater. Phys.* **2002**, *66*, 205319.

(58) Krstić, P. S.; Dean, D. J.; Zhang, X. G.; Keffer, D.; Leng, Y. S.; Cummings, P. T.; Wells, J. C. Computational chemistry for molecular electronics. *Comput. Mater. Sci.* **2003**, *28*, 321–341.

(59) Zhang, X. G.; Krstić, P. S.; Butler, W. H. Generalized tight-binding approach for molecular electronics modeling. *Int. J. Quantum Chem.* **2003**, *95*, 394–403.

(60) Ding, W.; Negre, C. F. A.; Vogt, L.; Batista, V. S. High-Conductance Conformers in Histograms of Single-Molecule Current–Voltage Characteristics. *J. Phys. Chem. C* **2014**, *118*, 8316–8321.

(61) Yin, X.; Li, Y.; Zhang, Y.; Li, P.; Zhao, J. Theoretical analysis of geometry-correlated conductivity of molecular wire. *Chem. Phys. Lett.* **2006**, *422*, 111–116.

(62) Li, Y.; Zhao, J.; Yin, X.; Yin, G. Ab Initio Investigations of the Electric Field Dependence of the Geometric and Electronic Structures of Molecular Wires. *J. Phys. Chem. A* **2006**, *110*, 11130–11135.

(63) Staykov, A.; Nozaki, D.; Yoshizawa, K. Theoretical Study of Donor– π –Bridge–Acceptor Unimolecular Electric Rectifier. *J. Phys. Chem. C* **2007**, *111*, 11699–11705.

(64) Pan, J. B.; Zhang, Z. H.; Deng, X. Q.; Qiu, M.; Guo, C. Rectifying performance of D- π -A molecules based on cyanovinyl aniline derivatives. *Appl. Phys. Lett.* **2010**, *97*, 203104.

(65) Pan, J. B.; Zhang, Z. H.; Deng, X. Q.; Qiu, M.; Guo, C. The transport properties of D- σ -A molecules: A strikingly opposite directional rectification. *Appl. Phys. Lett.* **2011**, *98*, 013503.

(66) Tsuji, Y.; Staykov, A.; Yoshizawa, K. Molecular Rectifier Based on π - π Stacked Charge Transfer Complex. *J. Phys. Chem. C* **2012**, *116*, 2575–2580.

(67) Lee, C.; Yang, W.; Parr, R. G. Development of the Colle-Salvetti correlation-energy formula into a functional of the electron density. *Phys. Rev. B: Condens. Matter Mater. Phys.* **1988**, *37*, 785–789.

(68) Frisch, M. J.; Trucks, G. W.; Schlegel, H. B.; Scuseria, G. E.; Robb, M. A.; Cheeseman, J. R.; Scalmani, G.; Barone, V.; Mennucci, B.; Petersson, G. A.; Nakatsuji, H.; Caricato, M.; Li, X.; Hratchian, H. P.; Izmaylov, A. F.; Bloino, J.; Zheng, G.; Sonnenberg, J. L.; Hada, M.; Ehara, M.; Toyota, K.; Fukuda, R.; Hasegawa, J.; Ishida, M.; Nakajima, T.; Honda, Y.; Kitao, O.; Nakai, H.; Vreven, T.; Montgomery, J. A., Jr.; Peralta, J. E.; Ogliaro, F.; Bearpark, M.; Heyd, J. J.; Brothers, E.; Kudin, K. N.; Staroverov, V. N.; Kobayashi, R.; Normand, J.; Raghavachari, K.; Rendell, A.; Burant, J. C.; Iyengar, S. S.; Tomasi, J.; Cossi, M.; Rega, N.; Millam, J. M.; Klene, M.; Knox, J. E.; Cross, J. B.; Bakken, V.; Adamo, C.; Jaramillo, J.; Gomperts, R.; Stratmann, R. E.; Yazyev, O.; Austin, A. J.; Cammi, R.; Pomelli, C.; Ochterski, J. W.; Martin, R. L.; Morokuma, K.; Zakrzewski, V. G.; Voth, G. A.; Salvador, P.; Dannenberg, J. J.; Dapprich, S.; Daniels, A. D.; Farkas, Ö.; Foresman, J. B.; Ortiz, J. V.; Cioslowski, J.; Fox, D. J. *Gaussian 09*, Gaussian, Inc.: Wallingford, CT, 2009.

(69) Hong, W.; Manrique, D. Z.; Moreno-García, P.; Gulcur, M.; Mishchenko, A.; Lambert, C. J.; Bryce, M. R.; Wandlowski, T. Single Molecular Conductance of Tolanes: Experimental and Theoretical Study on the Junction Evolution Dependent on the Anchoring Group. *J. Am. Chem. Soc.* **2012**, *134*, 2292–2304.

(70) Yang, Z.; Di Ventra, M. Nonlinear current-induced forces in Si atomic wires. *Phys. Rev. B: Condens. Matter Mater. Phys.* **2003**, *67*, 161311.

(71) Junquera, J.; Paz, Ó.; Sánchez-Portal, D.; Artacho, E. Numerical atomic orbitals for linear-scaling calculations. *Phys. Rev. B: Condens. Matter Mater. Phys.* **2001**, *64*, 235111.

(72) Perdew, J. P.; Burke, K.; Ernzerhof, M. Generalized Gradient Approximation Made Simple. *Phys. Rev. Lett.* **1996**, *77*, 3865–3868.

(73) Hihath, J.; Bruot, C.; Nakamura, H.; Asai, Y.; Díez-Pérez, I.; Lee, Y.; Yu, L.; Tao, N. Inelastic Transport and Low-Bias Rectification in a Single-Molecule Diode. *ACS Nano* **2011**, *5*, 8331–8339.

(74) Metzger, R. M. Unimolecular rectifiers: Methods and challenges. *Anal. Chim. Acta* **2006**, *568*, 146–155.